International Journal of GEOMATE, June., 2021, Vol.20, Issue 82, pp.153-160
ISSN: 2186-2982 (P), 2186-2990 (O), Japan, DOI: https://doi.org/10.21660/2021.82.j2106
Geotechnique, Construction Materials and Environment

HYDRAULIC COMPARISON BETWEEN PIANO KEY WEIR AND RECTANGULAR LABYRINTH WEIR

*Anh Tuan Le[1], Ken Hiramatsu[2], Tatsuro Nishiyama[2]

[1]The United Graduate School of Agricultural Science, Gifu University, Gifu, Japan;
[2]Faculty of Applied Biological Sciences, Gifu University, Gifu, Japan.

*Corresponding Author, Received: 04 Feb. 2021, Revised: 25 Feb. 2021, Accepted: 08 Mar. 2021

ABSTRACT: Nonlinear weirs, such as labyrinth and piano key weirs, are suitable methods to handle increased flood flows that may be expected due to climate change. Although specific physical models are considered to be an effective way of investigating fluid flows, simply conducting physical model tests is insufficient to fully comprehend the hydraulic and discharge characteristics of non-linear weirs. In this study, computational fluid dynamics algorithms have been used extensively to investigate complex flow physics instead of relying on reduced scale models. The discharge capacity of the piano key weir and the rectangular labyrinth weir is compared using a three-dimensional numerical model, which is validated by the available experimental data. The results confirm that piano key weir is more efficient than the rectangular labyrinth weir for a wide range of head water ratios. By analyzing the contribution of discharge over inlet, outlet and sidewall crests, the factor that make the piano key weir superior to the rectangular weir is the sidewall discharge.

Keywords: Computational fluid dynamics, Discharge coefficients, Numerical analysis, Piano key weir, Rectangular labyrinth weir

1. INTRODUCTION

The availability of hydrological and meteorological data coupled with new dam-safety guidelines have increased the Probable Maximum Flood (PMF), the Spillway Evaluation Flood (SEF), or the Inflow Design Flood (IDF) that a dam is required to pass [1]. One of the most common problems for obsolete dams is spillways that are no longer sufficient to handle updated flood flow due to climate change. If water cannot escape quickly enough through spillways, it could flow over the top of a dam, which would increase the likelihood of extensive erosion that can cause it to collapse [2].

Increased discharge capacity of an existing spillway can be achieved by increasing either the spillway crest length or discharge coefficient or operating head, or any combinations [3]. The operating head for a given spillway can be increased by either lowering the spillway crest and installing gates, or raising the dam crest to permit higher reservoir levels. However, adopting these approaches will lead to a great rise in costs of investment and operations management. A modest increase in the coefficient of discharge can generally be realized by reshaping the crest and by channel improvement, but at great cost. A more common modification to existing dam to accommodate larger floods is the enlargement of the spillway crest length without an associated increase in structure width, which is always limited by the layout of the discharge structures or site conditions.

Labyrinth weir is an especially suitable method which is employed to alleviate the problem of restricted spillway widths. Labyrinth spillways are polygonal overflow weirs folded in plan-view to provide a longer total crest length for a given overall spillway width. Although there are many geometric configurations of labyrinth weirs, three of them are widely used: triangular, trapezoidal and rectangular. Due to their polygonal shape, labyrinth weirs provide higher discharge capacity than linear overflow weirs for the same width and upstream energy head [4]. The best example is the labyrinth weir of the Beni Bahdel dam built in Algeria in 1938. Its approximate discharge capacity is 1200 m^3/s at a head of 0.5 m with the total crest length of 1200 m which is shrunk into a channel of 80 m width. At the same head (0.5 m), a traditional sharp-crested weir would discharge only 95 m^3/s [5]. Although labyrinth weirs may be very cost effective, they require a specific topography; this may explain their limited success [6–8].

Piano key (PK) weirs are a modified type of labyrinth weir that has rectangular cycles with overhangs and ramps in each cycle [6, 7]. The use of overhangs decreases the footprint of the structure (Fig. 1) and permits its installation on top of the existing structures such as gravity dams and embankment dams. Compared to a labyrinth weir, the inclined bottoms in the cycles of the PK weir help to reduce the lateral forces exerting on the side walls and hence the structural cost [9].

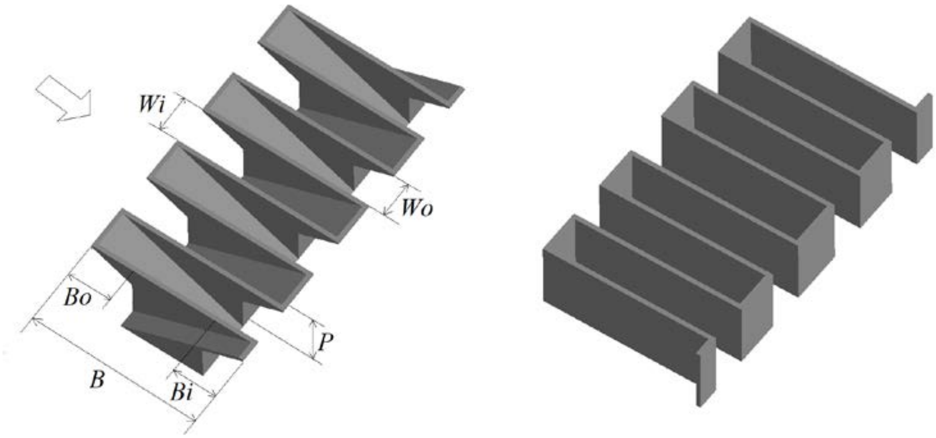

Fig.1 Piano Key weir (left) with geometrical parameters; Rectangular labyrinth weir (right)

A significant amount of research has been carried out during the last years to investigate the hydraulic behavior of labyrinth and PK weirs with three landmark international conferences [7, 10–15] but relatively few investigations on the topic of rectangular labyrinth (RL) weirs (side leg angel $\alpha = 0^o$). Tullis et al. [16] developed a comprehensive design procedure for trapezoidal labyrinth spillways estimating the discharge capacity with side leg angles of the weir varying from 6^o to 35^o. Machiels et al. [17] tested a large scale model to enhance the understanding of the flows over the PK weirs. Karimi et al. [18] studied the hydraulic characteristics of PK side weirs and emphasized the significant advantages of PK side weirs and rectangular labyrinth side weirs in terms of discharge capacity compared with conventional linear side weirs.

However, aforementioned studies used only scaled models based on similitude theory. Although specific physical models are considered to be an effective way of investigating fluid flows, simply conducting physical model tests is insufficient to fully comprehend the hydraulic and discharge characteristics of non-linear weirs. In recent years, advances in computing power and computational fluid dynamics (CFD) algorithms have been used extensively to investigate complex flow physics instead of relying on reduced scale models, and evaluate the design and operation of the non-linear weirs [14], [19–25]. Although some of those are preliminary studies without validation by physical models, their results showed that CFD approach has a promising future of weir investigations. For the more specific case of nonlinear weirs, there have been numerous hydraulic studies regarding discharge capacity but relatively few investigations on the topic of comparison between PK weir and RL weir.

The objectives of this study are:

1) to validate and verify a numerical model for determining the discharge capacity over the PK and RL weirs;

2) to compare the discharge efficiency of the PK and RL weirs;

3) to carry out a qualitative comparison between PK and RL weirs regarding to the discharge per unit length;

4) to develop a better understanding of the flow dynamics passing over the PK and RL weirs.

Therefore, to meet this need, this study was performed using numerical model with a wide range of the ratio of the upstream energy head and the weir height H/P ($0.15 \leq H/P \leq 0.75$) to compare discharge efficiency of PK and RL weirs.

2. METHODS

Numerical modeling to simulate the physical models is performed with a commercially available CFD software FLOW-3D that solves the Reynolds-Averaged Navier-Stokes (RANS) equations by the finite volume method. The program utilizes a true volume of fluid (true VOF) method to track the fluid surfaces or interfaces [26] and the fractional area/volume obstacle representation (FAVOR) technique to define complex geometric regions within the rectangular grid [27]. Herein, three of the most usual two-equation RANS turbulence models were tested: the standard k−ε model; the Re-Normalization Group (RNG) k−ε model; and the k−ω based Shear–Stress Transport (SST) model. In general, no remarkable differences were observed between the three turbulence models [28]. This may be because the discharge over the weirs is dominated by gravitational effects rather than by turbulence, for such geometric and hydraulic conditions. In this study, the k-ε turbulence closure model is used to account for turbulence effects. The conservation of mass and momentum equations in vector form with the FAVOR and VOF modification are:

$$\frac{\partial}{\partial x_i}\left(u_i A_i\right) = 0 \tag{1}$$

$$\frac{\partial u_i}{\partial t} + \frac{1}{V_F}\left(u_j A_j \frac{\partial u_i}{\partial x_j}\right) = -\frac{1}{\rho}\frac{\partial p}{\partial x_i} + g_i + f_i \tag{2}$$

where t is the time, u_i are the velocity components along the axes x, y and z, respectively, of a Cartesian coordinate system, p is the pressure, ρ is the density, and V_F is the fractional volume open to the flow. A_i, A_j are the fractional areas open to flow along x, y, and z, respectively, g_i are body accelerations along x, y, and z, respectively, and f_i are viscous accelerations along x, y, and z, respectively. The viscous accelerations include the Reynolds stresses.

The computational domain was constructed based on the experimental prototype of [4], i.e., a rectangular flume measuring 7.3 m long, 0.93 m wide, and 0.61 m deep, with the x, y, z axes in the streamwise, spanwise and height direction, respectively. The geometrical parameters for both types of the non-linear weirs are the same as Table 1, where P is weir height; W is total weir width; W_i is inlet key width; W_o is outlet key width; B is weir sidewall length; B_i is downstream or inlet key overhang length; B_o is upstream or outlet key overhang length; T_s is crest thickness; N is weir cycle number.

Although multi-block and/or nested meshes are an option, a single typical hexahedral mesh was chosen to minimize numerical interpolation and truncation at mesh block boundaries. An adaptive grid refinement method is presented to ensure the quality of the grid, which is always a critical issue in application of CFD.

The computational domain including boundary conditions, is shown in Fig. 2. A stagnation pressure (P) inlet condition was applied at the upstream plane. The top plane was set to the standard atmospheric pressure (P). For the downstream boundary, the domain should end up with a cross-section of supercritical flow, with an outflow condition (O). Wall condition (W) was applied at left and right planes and bottom plane of the channel. The wall boundary was treated as no-slip conditions.

In this study, the grid convergence index (GCI) was used to guarantee a grid independent solution. The GCI is not a direct measurement of the mesh accuracy; however, it provides a measure of uncertainty of the grid convergence, i.e. it indicates how much the solution would change with a further refinement of the grid. The smaller value of GCI shows, the nearer to the asymptotic range the computation is. With four-grid resolution, the factor of safety is recommended to be F_s = 1.25 [29].

To obtain an accurate simulation time-step size, a stability and convergence criterion is utilized. Furthermore, the flow kinetic energy, the flow rate at the outlet boundary and also the free surface elevation at the inlet boundary were defined in each numerical model. Based on the monitoring results, the simulations become fully converged and reach the steady-state condition after 15 seconds.

The calibration data provided by [4] have enabled the comparison between numerical and physical results on a large range of upstream head going from 0.03 m to 0.15 m. Discharge over PK weir can be expressed by standard weir Eq. (3):

$$Q = C_d W \sqrt{2gH_T^3} \quad (3)$$

where Q is flow discharge over weir; C_d is discharge coefficient, W is total width of the weir; g is the gravitational acceleration and H_T is upstream total head.

Table 1 Experimental detail dimensions

P (m)	W (m)	W_i (m)	W_o (m)	B (m)	B_i (m)	B_o (m)	T_s (m)	N
0.197	0.937	0.01	0.01	0.489	0.121	0.121	0.0127	4

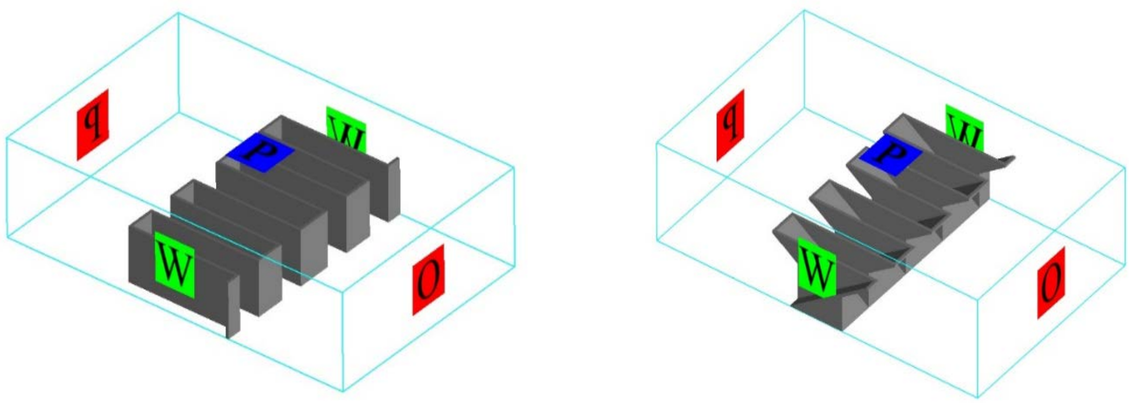

Fig. 2 Geometry of the RL weir (left) and PK weir (right) and boundary conditions

3. RESULTS AND DISCUSSION

3.1 Grid Convergence Calculation

For testing the mesh convergence, the GCI values were computed using the mesh sizes shown in Table 2. Similarly to [30], in this study, the total discharge capacity Q is used as the representative solution value, with GCI values lower than 1.0%. Considering the obtained results, a mesh based on 0.006 m hexahedral elements was considered sufficiently insensitive to be used in this study.

3.2 Numerical Model Validation

The numerical and experimental C_d results are plotted against the ratio of the upstream energy head and the weir height H/P in Fig. 3. The discharge coefficient C_d curves calculated by [15, 31–33], are also included for comparison.

The CFD simulation predicts the discharge coefficient with great accuracy. The maximum and average relative deviations between the simulated and observed values are 8.3% and 4.1%, respectively. By comparing the discharge coefficients in the simulation and the experiment, the accuracy and reliability of the numerical model are validated.

3.3 Discharge Comparison

Competing with the physical model, the numerical counterpart gives the opportunity for detailed evaluation of the discharge capacity along the crest for the RL and PK weirs and to identify easily the efficient parts of the upstream crest of the outlet, downstream crest of the inlet and sidewall.

Fig. 4 compares differences in total discharge capacity between two non-linear spillways and percentage of total discharge in the inlet, outlet and sidewall for various normalized heads of H/P ranging from 0.15 to 0.75 for each type of weir. This figure shows that hydraulic performance of the PK weir is more efficient than the RL weir for most of the upstream head range. For low heads (H/P = 0.15), PK and RL weirs have similar discharge capacity, while increasing the upstream head, PK weir becomes superior to RL weir. Geometrically speaking, the sidewall crest occupies over 80% of the total crest length compared to about 20% of total crest length occupied by upstream and downstream crests. The distribution of total discharge between upstream, downstream and sidewall is close to the geometrical overflowing crest length distribution for lower heads. When upstream head increases, the percentage of total discharge passing through the sidewall decreases considerably, from nearly 80% for H/P = 0.15 to 50% for H/P = 0.75.

Table 2 Grid convergence index (GCI) results

Grid size D (mm)	α (D_i/D_{i+1})	Q_{CFD} (l/s)	Relative error (δ)	GCI (%)
10	---	4.72	---	---
9	1.11	4.674	-0.00984	5.2
8	1.125	4.63	-0.0095	4.5
6	1.33	4.614	-0.00347	0.6

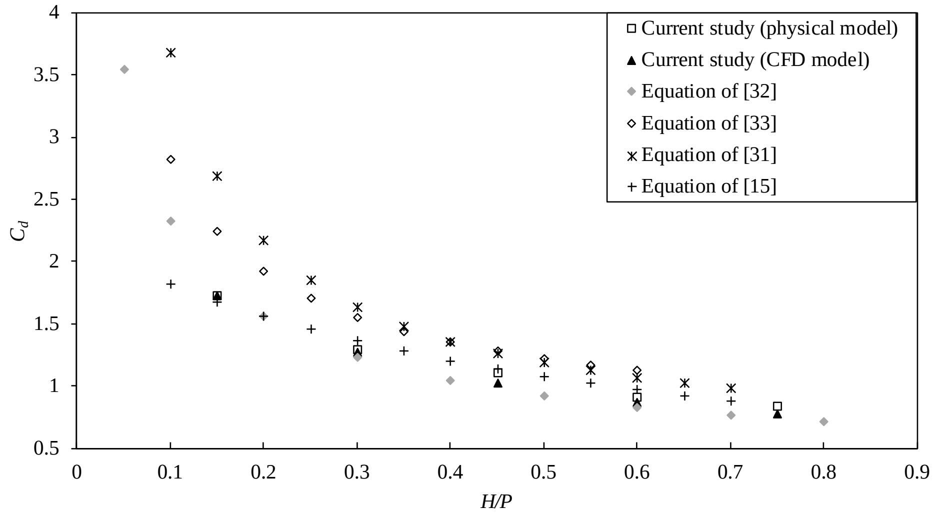

Fig. 3 Comparison of discharge coefficients estimated by equations of different authors with physical and CFD results

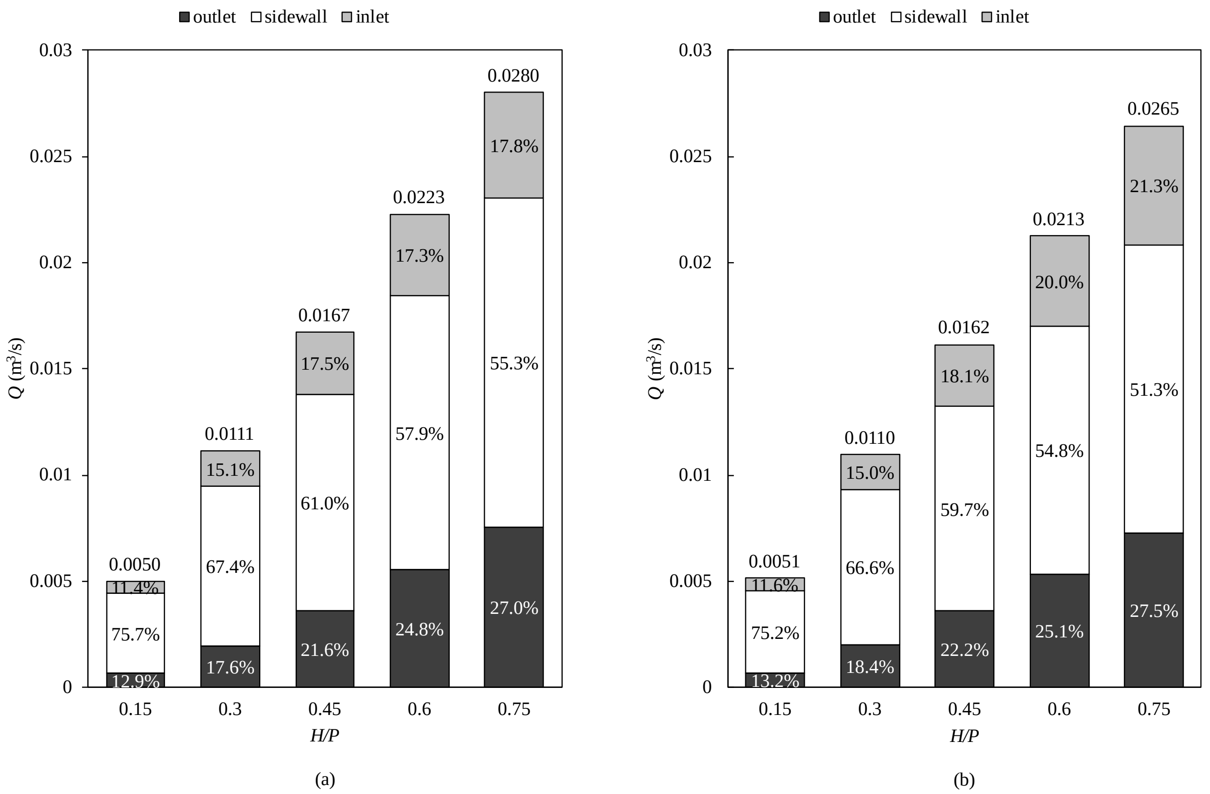

Fig. 4 Percentage of total discharge in the inlet, outlet and sidewall of (a) PK weir, (b) RL weir

3.4 Discharge Distribution

The results presented are based on discharge capacity comparisons. Because of the complexity of flow over the weirs and weirs geometry, hydraulic interpretation of the above mentioned results is an uneasy task. To accurately analyze the hydraulics of various tested weirs and also to determine the causes of the increase in PK weir discharge efficiency compared to the RL weir, a quantitative comparison has been made between PK weir and RL weir regarding the discharge per unit crest length. To determine the distribution, the developed crest on half of the unit considered has been defined using the curvilinear abscissa *S* (Fig. 5).

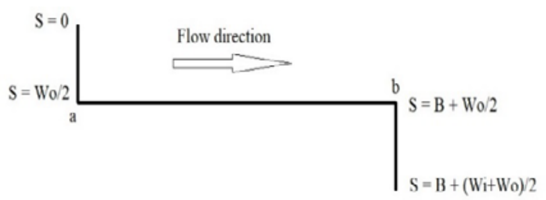

Fig.5 Curvilinear abscissa *S*

The numerical model used in this study allows the determination of the specific discharge along the crest. To do so, twenty-one juxtaposed flux surfaces were installed along the crest of each weir, and steady flow rate has been calculated for every baffle. A flux surface is one of available general history data in FLOW-3D for computing fluid flow rates. A typical flux surface is a 100% porous baffle with no flow losses, so it does not affect the flow in any way.

Fig. 6 compares specific discharge distribution along the crest of the various tested weirs. For RL weir, the specific discharge capacity curve performs an increasing trend along the sidewall crest, while for the PK weir, the discharge capacity remains constant for bulk of the sidewall crest. For both tested weirs, the minimum discharge per unit length is observed at the intersections of the sidewall with the upstream outlet key and downstream inlet key crests (position *a* and *b* in Fig. 5). There is no significant difference between discharge over upstream crest and downstream crest of both types of weir. The main factor that makes the PK weir more efficient than the RL weir is the sidewall discharge. Comparison between PK and RL weirs shows that the PK weir is more efficient along the first third of the sidewall for low head conditions (H/P = 0.15). However, as upstream water head H continues to rise, the RL weir sidewall becomes less effective. For example, when H/P > 0.6, specific discharge over sidewall of the PK weir is almost higher than the one over the sidewall of the RL weir.

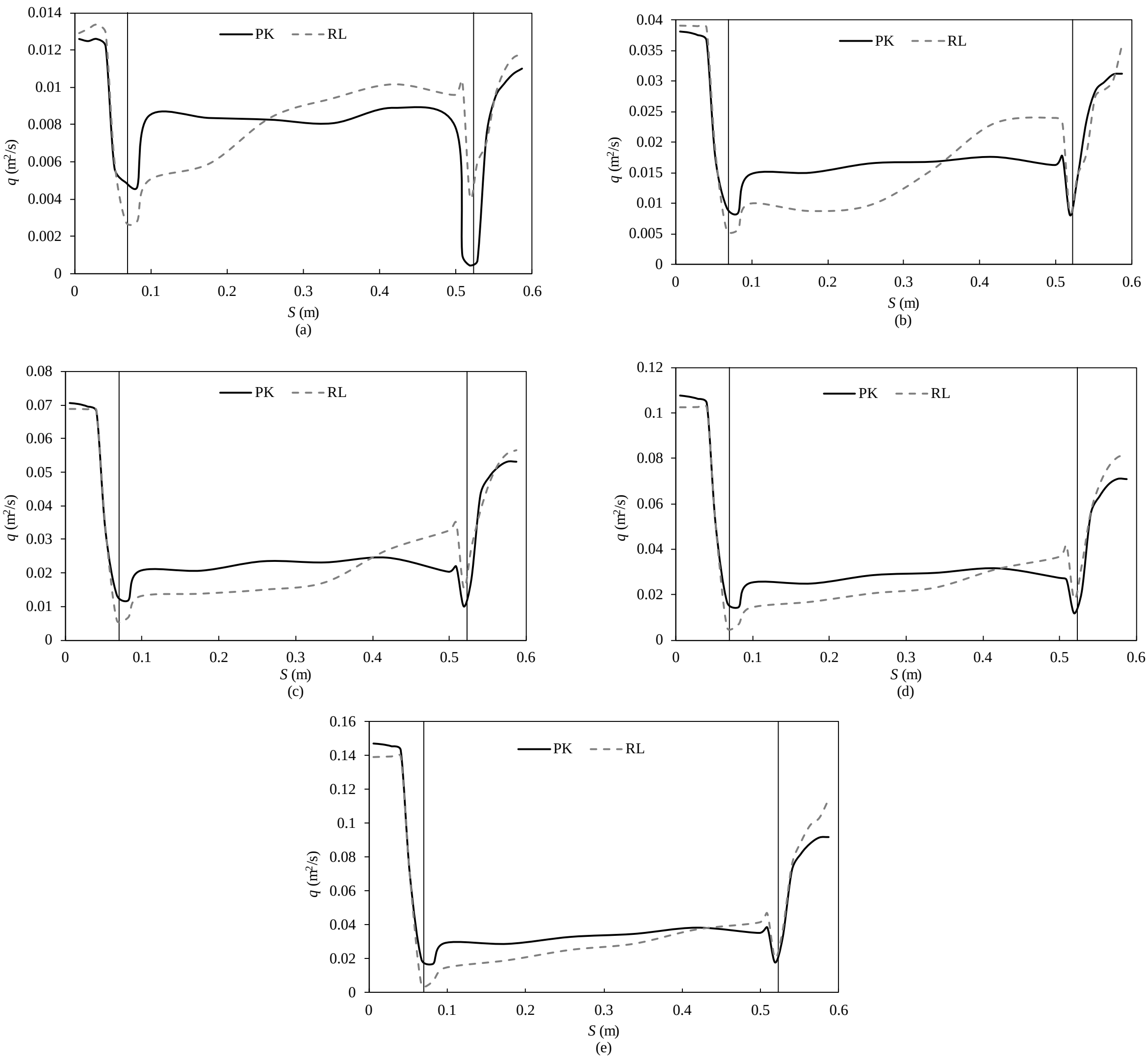

Fig. 6 Comparison between PK and RL weir flow rate distribution along the crest (a) H/P = 0.15; (b) H/P = 0.3; (c) H/P = 0.45; (d) H/P = 0.6; (e) H/P = 0.75

The detailed observation of the flow characteristics helps explain the advantages of PK weir compared to RL weir. Ripple pattern in the water surface profile is more obvious on RL weir (Fig. 7), indicating more significant flow contraction and energy loss condition. The water surface drop in PK weir is less than RL weir. This phenomenon partly explains why PK weir is more discharge efficient than the labyrinth type.

Furthermore, the local submergence of the RL is known as one of the behaviors having a major influence on the discharge decrease of the structure. The local submergence region occurs near the upstream crests of the outlet key and develops with upstream water head until the entire outlet key of the labyrinth weir eventually becomes submerged independent on the tail water elevation [34]. In addition to local submergence, other hydraulic byproducts of nappe collision include standing waves and wake in the outlet keys (Fig. 8). Meanwhile, the sloped floor in the outlet key of the PK weir helps to easier discharge of the released flow from the outlet crests, compared to RL weir. The gain for sidewall crest of the PK weir relative to the RL weir, as already shown in Fig. 6, can also be explained considering this phenomenon.

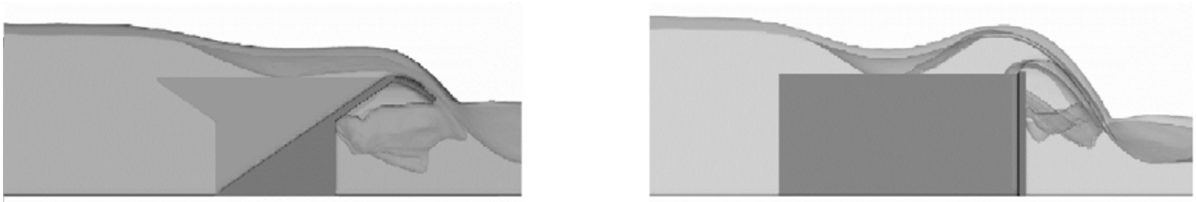

Fig. 7 Weir side section views (H/P = 0.45): PK weir (left); RL weir (right)

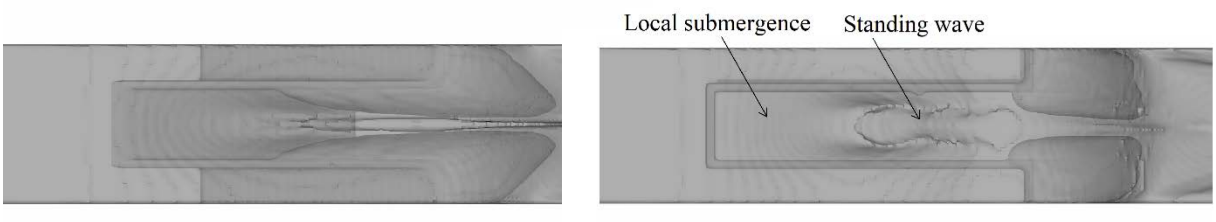

Fig. 8 Weir plan views (H/P = 0.45): PK weir (left); RL weir (right)

4. CONCLUSIONS

Experimental data were collected in this study to evaluate the performance of the numerical model. It was found that the numerical model has ability to predict the discharge capability of nonlinear weirs. Its accuracy was even higher than four of the most popular analytical equations used recent studies.

To compare the discharge efficiency of the PK and RL weir with the same developed crest lengths, three-dimensional free surface numerical simulations have been performed. The PK weir produced higher discharge capacity than all of the geometrical comparable RL weir, with the exception of small H/P. The PK weir maximum and average discharge efficiencies (quantified by C_d) for $0.3 \leq H/P \leq 0.75$ were respectively from 3,1 to 5,6% larger, in comparison to the RL weir.

Furthermore, using flux surfaces, variation of the discharge per unit length along the crest of the various tested weirs has been calculated, and the percentage contribution of the inlet, outlet and sidewall crests in the discharge capacity of the weirs has been determined. Based on the results of the numerical simulations, the reduction in discharge capacity of RL weir (relative to PK weir) is solely attributable to the colliding nappes flowing over two adjacent sidewall crests. This phenomenon is attributed to the sloped floors in the outlet key of the PW weir.

5. REFERENCES

[1] Felder G., Zischg A. and Weingartner R., The Effect Of Coupling Hydrologic And Hydrodynamic Models On Probable Maximum Flood Estimation, Journal of Hydrology, Vol. 550, 2017, pp. 157–165.

[2] Lempérière F., Dams And Floods, Engineering, Vol. 3, Number 1, 2017, pp. 144–149.

[3] Xlyang J. and Cederström M., Modification Of Spillways For Higher Discharge Capacity, Journal of Hydraulic Research, Vol. 45, Number 5, 2007, pp. 701–709.

[4] Anderson R.M., Piano Key Weir Head Discharge Relationships, Utah State University, 2011.

[5] Lempérière F. and Vigny J.P., General Comments On Labyrinths And Piano Key Weirs: The Past And Present, in *Labyrinth and Piano Key Weir - PKW 2011*, 2011, pp. 17–32.

[6] Blanc P. and Lempérière F., Labyrinth Spillways Have A Promising Future, International journal on hydropower and dams, Vol. 8, Number 4, 2001, pp. 129–131.

[7] Lempérière F. and Ouamane A., The Piano Keys Weir: A New Cost-Effective Solution For Spillways, International Journal on Hydropower and Dams, Vol. 10, Number 5, 2003, pp. 144–149.

[8] Bilhan O., Aydin M.C., Emiroglu M.E. and Miller C.J., Experimental And CFD Analysis Of Circular Labyrinth Weirs, Journal of Irrigation and Drainage Engineering, Vol. 144, Number 6, 2018, pp. 1–11.

[9] R. Eslinger K. and Crookston B.M., Energy Dissipation Of Type A Piano Key Weirs, Water, Vol. 12, Number 5, 2020, pp. 1253.

[10] Erpicum S., Laugier F., Ho Ta Khanh M. and Pfister M., Labyrinth And Piano Key Weirs III - PKW 2017, 2017.

[11] Erpicum S., Laugier F., Pfister M., Pirotton M., Cicero G. M. and Schleiss A. J., Labyrinth And Piano Keyweirs II – PKW 2013, 2013, pp. 292.

[12] Erpicum S., Laugier F., Boillat J.L., Pirotton M., Reverchon B. and Schleiss A., Labyrinth And Piano Key Weirs - PKW 2011, 2011, pp. 297.

[13] Crookston B.M., Erpicum S., Tullis B.P. and Laugier F., Hydraulics Of Labyrinth And Piano Key Weirs: 100 Years Of Prototype Structures, Advancements, And Future Research Needs, Journal of Hydraulic Engineering, Vol. 145, Number 12, 2019, pp. 1–7.

[14] Crookston B.M., Anderson R.M. and Tullis B.P., Free-Flow Discharge Estimation Method For Piano Key Weir Geometries, Journal of Hydro-Environment Research, Vol. 19, 2018, pp. 160–167.

[15] Machiels O., Pirotton M., Pierre A., Dewals B. and Erpicum S., Experimental Parametric Study And Design Of Piano Key Weirs, Journal of Hydraulic Research, Vol. 52, Number 3, 2014, pp. 326–335.

[16] Tullis J.P., Amanian N. and Waldron D., Design Of Labyrinth Spillways, Journal of Hydraulic Engineering, Vol. 121, Number 3, 1995, pp.

247–255.
[17] Machiels O., Erpicum S., Dewals B.J., Archambeau P. and Pirotton M., Experimental Observation Of Flow Characteristics Over A Piano Key Weir, Journal of Hydraulic Research, Vol. 49, Number 3, 2011, pp. 359–366.
[18] Karimi M., Attari J., Saneie M. and Ghazizadeh M.R.J., Side Weir Flow Characteristics: Comparison Of Piano Key, Labyrinth, And Linear Types, Journal of Hydraulic Engineering, Vol. 144, Number 12, 2018, pp. 1–13.
[19] Crookston B.M., Paxson G.S. and Savage B.M., Hydraulic Performance Of Labyrinth Weirs For High Headwater Ratios, 4th IAHR International Symposium on Hydraulic Structures, 9-11 February 2012, Porto, Portugal.
[20] Paxson G. and Savage B., Labyrinth Spillways: Comparison Of Two Popular U.S.A. Design Methods And Consideration Of Non-Standard Approach Conditions And Geometries, International Junior Researcher and Engineer Workshop on Hydraulic Structures, 2006, pp. 37–46.
[21] Li G., Li S. and Hu Y., The Effect Of The Inlet/Outlet Width Ratio On The Discharge Of Piano Key Weirs, Journal of Hydraulic Research, Vol. 58, Number 4, 2020, pp. 594-604.
[22] Crookston B.M., Crowley L. and Pfister M., Piano Key Weir For Enlargement Of The West Fork Of Eno River Reservoir, 6th International Symposium on Hydraulic Structures: Hydraulic Structures and Water System Management, ISHS 2016, Vol. 3300628160, 2016, pp. 430–439.
[23] Hu H., Qian Z., Yang W., Hou D. and Du L., Numerical Study Of Characteristics And Discharge Capacity Of Piano Key Weirs, Flow Measurement and Instrumentation, Vol. 62, Number May, 2018, pp. 27–32.
[24] Ghanbari R. and Heidarnejad M., Experimental And Numerical Analysis Of Flow Hydraulics In Triangular And Rectangular Piano Key Weirs, Water Science, 2020, pp. 1–7.
[25] Safarzadeh A. and Noroozi B., 3D Hydrodynamics Of Trapezoidal Piano Key Spillways, International Journal of Civil Engineering, Vol. 15, Number 1, 2017, pp. 89–101.
[26] Hirt C.W. and Nichols B.D., Volume Of Fluid (VOF) Method For The Dynamics Of Free Boundaries, Journal of Computational Physics, Vol. 39, Number 1, 1981, pp. 201–225.
[27] Hirt C.W. and Sicilian J.M., A Porosity Technique For The Definition Of Obstacles In Rectangular Cell Meshes, International Conference on Numerical Ship Hydrodynamics, 4th, 1985.
[28] Pralong J., Montarros F., Blancher B. and Laugier F., A Sensitivity Analysis Of Piano Key Weirs Geometrical Parameters Based On 3D Numerical Modeling, Labyrinth and Piano Key Weirs - Proceedings of the International Conference on Labyrinth and Piano Key Weirs, PKW 2011, 2011, pp. 133–139.
[29] Roache P.J., Quantification Of Uncertainty In Computational Fluid Dynamics, Annual Review of Fluid Mechanics, Vol. 29, Number 1, 1997, pp. 123–160.
[30] Savage B.M., Crookston B.M. and Paxson G.S., Physical And Numerical Modeling Of Large Headwater Ratios For A 15° Labyrinth Spillway, Journal of Hydraulic Engineering, Vol. 142, Number 11, 2016, pp. 461-467.
[31] Leite Ribeiro M., Pfister M., Schleiss A. J. and Boillat J. L., Hydraulic Design Of A-Type Piano Key Weirs, Journal of Hydraulic Research, Vol. 50, Number 4, 2012, pp. 400–408.
[32] Lempérière F., New Labyrinth Weirs Triple The Spillways Discharge, 2009,[Online]. Available: http://www.hydrocoop.org/new-labyrinth-weirs-triple-the-spillways-discharge/.
[33] Kabiri-Samani A. and Javaheri A., Discharge Coefficients For Free And Submerged Flow Over Piano Key Weirs, Journal of Hydraulic Research, Vol. 50, Number 1, 2012, pp. 114–120.
[34] Crookston B.M. and Tullis B.P., Labyrinth Weirs: Nappe Interference And Local Submergence, Journal of Irrigation and Drainage Engineering, Vol. 138, Number 8, 2012, pp. 757–765.